

Multiple induced transparency in a hybrid driven cavity optomechanical device with a two-level system

Wei Zhang(张伟), Li-Guo Qin(秦立国), Li-Jun Tian(田立君), and Zhong-Yang Wang(王中阳)
Citation: Chin. Phys. B, 2021, 30 (**9**): 094203. DOI: 10.1088/1674-1056/abf642
Journal homepage: http://cpb.iphy.ac.cn; http://iopscience.iop.org/cpb

What follows is a list of articles you may be interested in

Dissipative quantum phase transition in a biased Tavis-Cummings model

Zhen Chen(陈臻), Yueyin Qiu(邱岳寅), Guo-Qiang Zhang(张国强), Jian-Qiang You(游建强)
Chin. Phys. B, 2020, 29 (**4**): 044201. DOI: 10.1088/1674-1056/ab7b55

Analytic solutions for generalized *PT*-symmetric Rabi models

Yuanhao Dong(董元浩), Wen-Jing Zhang(张文静), Jing Liu(刘静), Xiao-Tao Xie(谢小涛)
Chin. Phys. B, 2019, 28 (**11**): 114202. DOI: 10.1088/1674-1056/ab457b

Modulation of energy spectrum and control of coherent microwave transmission at single-photon level by longitudinal field in a superconducting quantum circuit

Xueyi Guo(郭学仪), Hui Deng(邓辉), Hekang Li(李贺康), Pengtao Song(宋鹏涛), Zhan Wang(王战), Luhong Su(苏鹭红), Jie Li(李洁), Yirong Jin(金贻荣), Dongning Zheng(郑东宁)
Chin. Phys. B, 2018, 27 (**7**): 074206. DOI: 10.1088/1674-1056/27/7/074206

Triple optomechanical induced transparency in a two-cavity system

Shi-Chao Wu(吴士超), Li-Guo Qin(秦立国), Jun Jing(景俊), Guo-Hong Yang(杨国宏), Zhong-Yang Wang(王中阳)
Chin. Phys. B, 2016, 25 (**5**): 054203. DOI: 10.1088/1674-1056/25/5/054203

Multi-level effects in the high-order harmonic generation driven by intense frequency-comb laser fields

Zhao Di, Jiang Chen-Wei, Li Fu-Li
Chin. Phys. B, 2015, 24 (**7**): 074205. DOI: 10.1088/1674-1056/24/7/074205

Multiple induced transparency in a hybrid driven cavity optomechanical device with a two-level system*

Wei Zhang(张伟)[1], Li-Guo Qin(秦立国)[2,3,†], Li-Jun Tian(田立君)[1,‡], and Zhong-Yang Wang(王中阳)[3]

[1] *Department of Physics, Shanghai University, Shanghai* 200444, *China*
[2] *School of Mathematics, Physics and Statistics, Shanghai University of Engineering Science, Shanghai* 201620, *China*
[3] *Shanghai Advanced Research Institute, Chinese Academy of Sciences, Shanghai* 201210, *China*

(Received 31 December 2020; revised manuscript received 6 April 2021; accepted manuscript online 9 April 2021)

We present a scheme with the multiple-induced transparency windows in a hybrid optomechanical device. By studying the transmission of a probe field through the hybrid device, we show the successive generations of three transparent windows induced by multiple factors including tunneling, optomechanical and qubit-phonon coupling interactions, and analyze the physical mechanism of the induced transparency based on a simplified energy-level diagram of the system. Moreover, the effects of the transition frequency and decay rate of the two-level system on the multiple-induced transparency windows are discussed. We find that the transparency windows can be modulated by the coupling interaction between the qubit and NMR, the decay of qubit and the power of the control field. Therefore, the transmission of the probe field can be coherently adjusted in the hybrid cavity optomechanical device with a two-level system.

Keywords: hybrid optomechanical device, optomechanical induced transparency, two-level system

PACS: 42.50.Pq, 42.15.Eq, 07.10.Cm **DOI:** 10.1088/1674-1056/abf642

1. Introduction

As an excellent candidate for studying the transform of a macroscopic degree of freedom from the classical to the quantum regimes, cavity optomechanics composed of an Fabry–Pérot (FP) cavity with its end-mirror replaced by a nanomechanical resonator (NMR) has received considerable attention over the last decade.[1–5] In this emerging field, remarkable progress has been made in both theory and experiment, including quantum ground-state cooling of NMR,[6–8] slowing and storage of the light pulse,[9–11] information processing,[12–14] and optomechanical induced transparency (OMIT).[15–21]

When a strong control field and a weak probe field are applied to an optomechanical cavity, an optomechanical interference can lead to generation of OMIT, which has been reported theoretically[17] and then demonstrated experimentally.[22] Some exciting phenomena including the tunable slow and fast light,[23,24] four-wave mixing,[25] electro-optic interconnect[26] and squeezing of the mechanical model in the resolved sideband regime have been proposed based on the mechanism of OMIT.[27–29]

As a preferred component in the construction of complex quantum systems, NMR with the wide frequency range is a promising candidate to explore various applications of quantum behavior.[30–32] To find the properties and applications of NMR in the quantum region, it can be combined with other quantum systems to form hybrid systems, such as optomechanical systems[33,34] and quantum electromechanical systems.[14] A two-level system (for example, superconducting qubit, quantum dot and the inherent defect in materials) can also be embedded in NMR to study various quantum phenomena, such as controllable coupling,[35,36] quantum entanglement[37] and phonon blockade.[38] As a two-level system, the defect inside the NMR can interact with the NMR through the deformation force. Especially, when the transition frequency of an intrinsic two-level defect inside NMR is near resonance with the NMR frequency, the great effects of the defect on the quantum properties of NMR should not be ignored.[39–42]

Motivated by recent progress of two-level systems in optomechanical devices, here we study the interaction between a two-level system and a hybrid optomechanical device. Our model consists of an FP cavity tunneling coupled to an optomechanical cavity, where the two-level system is embedded in the movable cavity mirror of the optomechanical cavity. The two-level system can be considered as a defect inside the material of the movable cavity mirror or a superconducting charge qubit. The movable cavity mirror can be viewed as an NMR, which is coupled to the two-level system via the Jaynes–Cummings coupling. In this hybrid optomechanical system, we find the multiple optomechanically induced transparency and discuss the effects of two-level system on OMIT.

The paper is organized as follows. In Section 2, we describe the model by an effective Hamiltonian and give

*Project supported by the National Natural Science Foundation of China (Grant Nos. 61605225 and 11704238) and the Natural Science Foundation of Shanghai, China (Grant No. 16ZR1448400).

†Corresponding author. E-mail: lgqin@foxmail.com
‡Corresponding author. E-mail: tianlijun@shu.edu.cn

© 2021 Chinese Physical Society and IOP Publishing Ltd

Langevin motion equations and their stable solutions. In Section 3, a profile of multiple OMIT windows of the output field is presented. In Section 4, we discuss the effect of the qubit (two-level system) on the OMIT. A conclusion is given in Section 5.

2. Model and quantum Langevin equations

As schematically shown in Fig. 1(a), our model consists of an optical cavity a_1 tunneling-connected to an optomechanical cavity a_2, where as a moveable mirror of the optomechanical cavity, NMR b mechanically couples to a two-level system. The optical cavity a_1 is driven by a strong control field ε_c with frequency ω_c and a weak probe field ε_p with frequency ω_p. The two cavity fields are coupled via the photon tunneling interaction with the coupling strength J. The NMR with the frequency ω_m is coupled to the optomechanical cavity a_2 by the radiation pressure with the optomechanical coupling strength χ.

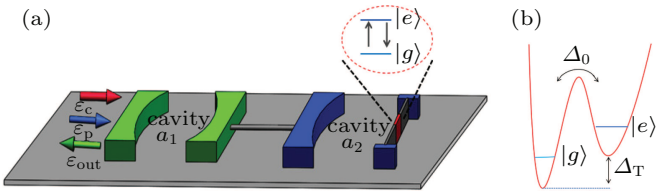


Fig. 1. (a) Schematic diagram of a hybrid optomechanical system. The optomechanical cavity a_2 with frequency ω_{a2} is coupled to the optical cavity a_1 with frequency ω_{a1} (via the tunneling interaction) and to the NMR (via the optomechanical coupling). As a two-level system, superconducting qubit or a defect is embedded inside the NMR, where $|g\rangle$ and $|e\rangle$ denote the ground and excited states, respectively. The hybrid optomechanical system is driven by a strong control field with the frequency ω_c and a weak probe field with the frequency ω_p. (b) The double-well potential model for the two-level system. Δ_0 and Δ_T are tunnel splitting frequency and the asymmetry frequency in the double-well potential, respectively.

In our model the intrinsic defect inside NMR or a superconducting charge qubit attached on NMR can be effectively described by the two-level state in a double-well potential at low temperature, as shown in Fig. 1(b). It is worth noting that the frequency gap of two energy levels is resonant or near-resonant with the frequency of the NMR, and the other energy levels are highly detuned with the frequency of the NMR, i.e., two-level approximation. For an isolated two-level system and the single mechanical mode of NMR, the Hamiltonian reads

$$H_0 = \hbar\omega_m b^\dagger b + \frac{1}{2}\hbar\Delta_T\bar{\sigma}_z + \frac{1}{2}\hbar\Delta_0\bar{\sigma}_x, \tag{1}$$

where b ($b^\dagger$) is the annihilation (creation) operator of the NMR, $\bar{\sigma}_{x,z}$ are the Pauli matrices. In Fig. 1(b), the asymmetry frequency Δ_T depends on the strain in the material and the NMR displacement generates a strain tensor at the position of the defect, so the two-level defect in the NMR can be coupled to the localized NMR. Under the action of external strain S and electric fields $\boldsymbol{E}_0$, the asymmetry frequency $\Delta_T(S,\boldsymbol{E}_0) \approx \Delta_T + 2D_T S + 2\boldsymbol{p}\cdot\boldsymbol{E}_0$, where D_T and $\boldsymbol{p}$ are the deformation potential tensor and the intrinsic electric dipole moment of the two-level system, respectively. The relations of external field coupling to the defect have been studied in detail in supplemental information of Ref. [40]. In our model, the optomechanical force induces the motion of NMR with the effective mass m_{eff} to generate the strain. The displacement of NMR can be quantized as $x = \sqrt{\frac{\hbar}{2m_{eff}\omega_m}}(b+b^\dagger)$. As a result, in the Heisenberg picture the strain can be given as $S(x,t) = S_{zpf}s(x)(b\,e^{-i\omega_m t} + b^\dagger e^{i\omega_m t})$, where $S_{zpf} = \sqrt{\frac{\hbar\omega_m}{2EV_m}}$ is the zero-point strain fluctuation with Young's modulus E of the material and the mode volume V_m of the mechanical mode, and $s(x)$ is a normalized strain profile of the interesting mode. We are interested in the situation: the effective transition frequency of the two-level system $\omega_q = \sqrt{\Delta_T^2 + \Delta_0^2} \approx \omega_m$, i.e., the transition frequency of two-levels system is near-resonant with the frequency of the NMR. When $E_0 = 0$, the Hamiltonian (1) can be rewritten in the Schrödinger picture as[39,40]

$$H_0 = \hbar\omega_m b^\dagger b + \left[\frac{1}{2}\hbar\Delta_T + \hbar\lambda(b^\dagger + b)\right]\bar{\sigma}_z + \frac{1}{2}\hbar\Delta_0\bar{\sigma}_x, \tag{2}$$

where the coupling strength $\lambda = \frac{D_T s(x)}{\hbar}\sqrt{\frac{\hbar\omega_m}{2EV_m}}$ depends on the deformation potential and the second-order derivative of the NMR displacement. For the convenience of discussion, we transform the eigenbasis of the system to the eigenbases of the uncoupled two-level system, that is, make the rotation change:[39–41]

$$\begin{bmatrix}\bar{\sigma}_z\\ \bar{\sigma}_x\end{bmatrix} = \begin{pmatrix}\cos\theta & -\sin\theta\\ \sin\theta & \cos\theta\end{pmatrix}\begin{bmatrix}\sigma_z\\ \sigma_x\end{bmatrix},$$

where $\cos\theta = \Delta_T/\omega_q$ and $\sin\theta = \Delta_0/\omega_q$. Equation (2) can be transformed to

$$H_0 = \hbar\omega_m b^\dagger b + \frac{\hbar\omega_q}{2}\sigma_z + \hbar g(b+b^\dagger)(\sigma_+ + \sigma_-), \tag{3}$$

where $g = \lambda\sin\theta$ denotes the effective coupling strength between the NMR and the two-level system, and $\sigma_-(\sigma_+)$ is the lowering (raising) operator for the two-level system. Making use of the rotating-wave approximation to omit counter-rotating terms, the Hamiltonian in Eq. (3) can be rewritten as[16,39,40,43,44]

$$H_{JC} = \hbar\omega_m b^\dagger b + \frac{\hbar\omega_q}{2}\sigma_z + \hbar g(b\sigma_+ + b^\dagger\sigma_-). \tag{4}$$

The first and second terms in Eq. (2) describe the energies of the NMR and qubit, respectively. The last term in Eq. (4) describes the JC-type coupling interactions between the two-level system and the NMR. In summary, for the JC-type coupling the following realizable physical conditions should be met: (a) The two-level system and the NMR are in near resonance, and are far-resonance with the cavity field. (b) The two-well potential satisfies the two-level approximation condition. (c) The conditions of the rotating-wave approximation,

i.e., the fast oscillation term of far-resonance, can be ignored. (d) Only consider the effects of the strain on the asymmetry frequency from NMR. Thus, the total Hamiltonian of the hybrid system in the rotating frame can be given by

$$\begin{aligned} H =\ & \hbar\Delta_1 a_1^\dagger a_1 + \hbar\Delta_2 a_2^\dagger a_2 + \hbar J(a_1^\dagger a_2 + a_2^\dagger a_1) \\ & - \hbar\chi a_2^\dagger a_2 (b^\dagger + b) + H_{\rm JC} + H_{\rm dr}, \end{aligned} \tag{5}$$

where the detunings $\Delta_{1(2)} = \omega_{\rm a1(2)} - \omega_{\rm c}$, a_i is the annihilation operators of the i-th cavity field with the decay rate κ_i ($i = 1, 2$), respectively. The third and fourth terms in Eq. (5) describe the coupling interactions between the two cavities, the optomechanical cavity a_2 and the NMR, respectively. The driven Hamiltonian $H_{\rm dr}$ can be written as

$$H_{\rm dr} = {\rm i}\hbar\varepsilon_{\rm c}(a_1^\dagger - a_1) + {\rm i}\hbar\varepsilon_{\rm p}(a_1^\dagger {\rm e}^{-{\rm i}\Delta t} - a_1 {\rm e}^{{\rm i}\Delta t}), \tag{6}$$

with $\Delta = \omega_{\rm p} - \omega_{\rm c}$. Here, $\varepsilon_{\rm c,p} = \sqrt{\frac{2\kappa_1 P_{\rm c,p}}{\hbar\omega_{\rm c,p}}}$ are the intensities of both input fields with the power $P_{\rm c,p}$.

From the Hamiltonian (5), the evolution of the system is determined by the quantum Langevin equations, which can be given as follows:

$$\begin{aligned} \dot{a}_1 &= -({\rm i}\Delta_1 + \kappa_1)a_1 - {\rm i}Ja_2 + \varepsilon_{\rm c} + \varepsilon_{\rm p}{\rm e}^{-{\rm i}\Delta t} + \sqrt{2\kappa_1}a_{1,{\rm in}}(t), \\ \dot{a}_2 &= -({\rm i}\Delta_2 + \kappa_2)a_2 - {\rm i}Ja_1 + {\rm i}\chi a_2(b^\dagger + b) + \sqrt{2\kappa_2}a_{2,{\rm in}}(t), \\ \dot{b} &= -({\rm i}\omega_{\rm m} + \gamma_{\rm m})b + {\rm i}\chi a_2^\dagger a_2 - {\rm i}g\sigma_- + \sqrt{2\gamma_{\rm m}}b_{\rm in}(t), \\ \dot{\sigma}_- &= -\left({\rm i}\omega_{\rm q} + \frac{\gamma_{\rm q}}{2}\right)\sigma_- + {\rm i}gb\sigma_z + \sqrt{\Gamma_-}(t), \\ \dot{\sigma}_z &= -\gamma_{\rm q}(\sigma_z + 1) - 2{\rm i}g(b\sigma_+ - b^\dagger\sigma_-) + \sqrt{\Gamma_z}(t), \end{aligned} \tag{7}$$

where $\gamma_{\rm m}$ and $\gamma_{\rm q}$ are the decay rates of the NMR and qubit, respectively. The operators $a_{1(2),{\rm in}}(t)$, $b_{\rm in}(t)$, $\Gamma_-(t)$ and $\Gamma_z(t)$ denote the zero-mean environment noises corresponding to the two cavities fields, the NMR and the two-level system, respectively. In order to solve the nonlinear equations, the mean field approximation $\langle AB\rangle = \langle A\rangle\langle B\rangle$ is used here, where A and B are two arbitrary operators. By the linear way, each operator can be split as a sum of its steady-state value and an additional small fluctuation operator, i.e., $O = O_{\rm s} + \delta O$ ($O = a_{1,2}, b, \sigma_-$ and σ_z). $O_{\rm s}$ corresponds to the stable solution of O, when the strong driving fields applied to the system; δO denotes the first order fluctuation operator of the injected weak field $\varepsilon_{\rm p}$. With these approximations, the steady-state values can be calculated by

$$\begin{aligned} a_{1,{\rm s}} &= \frac{-(\Delta_2' - {\rm i}\kappa_2)a_{2,{\rm s}}}{J}, \\ a_{2,{\rm s}} &= \frac{{\rm i}J\varepsilon_{\rm c}}{(\Delta_1 - {\rm i}\kappa_1)(\Delta_2' - {\rm i}\kappa_2) - J^2}, \\ b_{\rm s} &= \frac{{\rm i}\chi(\frac{\gamma_{\rm q}}{2} + {\rm i}\omega_{\rm q})|a_{2,{\rm s}}|^2}{(\gamma_{\rm m} + {\rm i}\omega_{\rm m})(\frac{\gamma_{\rm q}}{2} + {\rm i}\omega_{\rm q}) - g^2\sigma_{z,{\rm s}}}, \\ \sigma_{-,{\rm s}} &= \frac{{\rm i}gb_{\rm s}\sigma_{z,{\rm s}}}{\frac{\gamma_{\rm q}}{2} + {\rm i}\omega_{\rm q}}, \end{aligned}$$

$$\sigma_{z,{\rm s}} = -\frac{\omega_{\rm q}^2 + (\frac{\gamma_{\rm q}}{2})^2}{\omega_{\rm q}^2 + (\frac{\gamma_{\rm q}}{2})^2 + 2g^2|b_{\rm s}|^2}, \tag{8}$$

where $\Delta_2' = \Delta_2 - \chi(b_{\rm s} + b_{\rm s}^*)$ is the effective optomechanical detuning of the optomechanical cavity a_2. The optomechanical system is considered in the resolved sideband regime $\omega_{\rm m} \gg \kappa_2$ and the red sideband regime $\Delta_2' = \omega_{\rm m}$. To enhance the tunneling coupling between two cavity fields, two cavity modes are near resonant, i.e., $\Delta_1 = \omega_{\rm m}$. The NMR has a high nanomechanical quality factor $\omega_{\rm m} \gg \gamma_{\rm m}$ and resonates with qubit, i.e., $\omega_{\rm q} = \omega_{\rm m}$. By redefining $\langle\delta O\rangle = \delta O_+ {\rm e}^{-{\rm i}\Delta t}$, the equations of motion for the fluctuations can be rewritten as

$$\begin{aligned} \delta\dot{a}_{1_+} &= -(\kappa_1 - {\rm i}x)\delta a_{1_+} - {\rm i}J\delta a_{2_+} + \varepsilon_{\rm p}, \\ \delta\dot{a}_{2_+} &= -(\kappa_2 - {\rm i}x)\delta a_{2_+} - {\rm i}J\delta a_{1_+} + {\rm i}G\delta b_+, \\ \delta\dot{b}_+ &= -(\gamma_{\rm m} - {\rm i}x)\delta b_+ + {\rm i}G^*\delta a_{2_+} - {\rm i}g\delta\sigma_{-_+}, \\ \delta\dot{\sigma}_{-_+} &= -\left(\frac{\gamma_{\rm q}}{2} - {\rm i}x\right)\delta\sigma_{-_+} + {\rm i}gb_{\rm s}\delta\sigma_{z_+} + {\rm i}g\delta b\sigma_{z,{\rm s}}, \\ \delta\dot{\sigma}_{z_+} &= -(\gamma_{\rm q} - {\rm i}\Delta)\sigma_z + 2{\rm i}gb_{\rm s}^*\delta\sigma_{-_+} - 2{\rm i}g\delta b\sigma_{-,{\rm s}}^*, \end{aligned} \tag{9}$$

where $x = \Delta - \omega_{\rm m}$. $G = \chi a_{2{\rm s}}$ is the effective optomechanical coupling strength between the optical model a_2 and the NMR. Under the steady-state conditions of $\langle\delta\dot{O}_+\rangle = 0$, the solution of the intracavity field δa_{1_+} can be derived as

$$\delta a_{1_+} = \frac{\varepsilon_{\rm p}}{\kappa_1 - {\rm i}x + \dfrac{J^2}{\kappa_2 - {\rm i}x + \dfrac{|G|^2}{\gamma_{\rm m} - {\rm i}x + \frac{-g^2\sigma_{z,{\rm s}}(\gamma_{\rm q} - {\rm i}\Delta) + 2{\rm i}g^3 b_{\rm s}\sigma_-^*}{(\frac{\gamma_{\rm q}}{2} - {\rm i}x)(\gamma_{\rm q} - {\rm i}\Delta) - 2g^2|b_{\rm s}|^2}}}}. \tag{10}$$

The response of the system can be detected by the output field at the probe frequency $\omega_{\rm p}$. Based on the input-output relation $\varepsilon_{\rm out} + \varepsilon_{\rm c}{\rm e}^{-{\rm i}\omega_{\rm c}t} + \varepsilon_{\rm p}{\rm e}^{-{\rm i}\omega_{\rm p}t} = 2\kappa_1 a_1$, where $\varepsilon_{\rm out} = \varepsilon_{\rm outs} + \varepsilon_{\rm out_+}{\rm e}^{-{\rm i}\omega_{\rm p}t}$ and $a_1 = a_{1{\rm s}} + \delta a_{1_+}{\rm e}^{-{\rm i}\omega_{\rm p}t}$, we can obtain[15,45–47]

$$\varepsilon_{\rm out} = (2\kappa_1 a_{1{\rm s}} - \varepsilon_{\rm c}){\rm e}^{-{\rm i}\omega_{\rm c}t} + (2\kappa_1\delta a_{1_+} - \varepsilon_{\rm p}){\rm e}^{-{\rm i}\omega_{\rm p}t}. \tag{11}$$

Here, the first term in Eq. (11) on the right side corresponds to the output field at the control field frequency $\omega_{\rm c}$. The second term corresponds to the output field at the probe field frequency $\omega_{\rm p}$. We are interested in the output field at the probe field frequency, therefore we can define the transmission of the probe field as

$$\varepsilon_{\rm T} = \frac{\varepsilon_{\rm out_+}}{\varepsilon_{\rm p}} + 1 = \frac{2\kappa_1\delta a_{1_+}}{\varepsilon_{\rm p}} = \nu_{\rm p} + {\rm i}\tilde{\nu}_{\rm p}, \tag{12}$$

where $\nu_{\rm p} = {\rm Re}(\varepsilon_{\rm T})$ and $\tilde{\nu}_{\rm p} = {\rm Im}(\varepsilon_{\rm T})$ describe the absorption and dispersion of the whole system at the probe frequency, respectively.

3. The multiple induced transparency windows profile in the output field

In this section, we numerically study the transmission of a weak probe field through a hybrid optomechanical system. The parameters we used in the simulation[16,45] are $\omega_m/2\pi = \omega_q/2\pi = 51.8$ MHz, $\kappa_1/2\pi = 15.0$ MHz, $\kappa_2/2\pi = 1.5$ MHz, $\gamma_m/2\pi = 41.0$ kHz, $\gamma_q/2\pi = 51.8$ kHz, $J/2\pi = 15.0$ MHz, $\chi/2\pi = 2.16$ kHz, and $g/2\pi = 10.0$ MHz.

In order to more intuitively show the interactions in the hybrid system and to better understand the physical meaning of our results, the energy level diagram of the model is plotted as shown in Fig. 2. We can find that there are three interaction relationships associated with the different subsystem in our model, i.e., the tunneling coupling interaction between the two cavities, the optomechanical interaction between the cavity and the NMR, and the JC coupling interaction between the qubit and NMR. Next, we study the effects of three interactions on the output probe field.

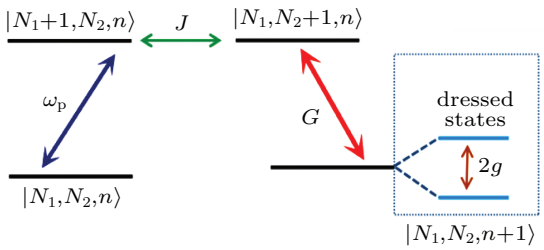


Fig. 2. Energy-level diagram of the hybrid system. The number state of the cavity i-th photons and phonons are denoted by N_i and n. The tunneling coupling strength between $|N_1+1,N_2,n\rangle$ and $|N_1,N_2+1,n\rangle$ is J; the effective optomechanical coupling strength between $|N_1,N_2+1,n\rangle$ and $|N_1,N_2,n+1\rangle$ is G; and the qubit–NMR coupling strength is g.

First, we assume that the tunnel-coupling strength between two cavities is negligible, i.e., $J = 0$, only transition $|N_1,N_2,n\rangle \leftrightarrow |N_1+1,N_2,n\rangle$ exists in Fig. 2. The absorption of the probe field shows a single Lorentzian shape because there is no quantum interference in the cavity field, as shown in Fig. 3(a). However, with the tunneling coupling ($J \neq 0$) and without the optomechanical interaction ($\chi = 0$), the transition $|N_1+1,N_2,n\rangle \leftrightarrow |N_1,N_2+1,n\rangle$ is additionally driven. The absorption peak of the output probe field is split due to photon hopping between two cavities, which leads to the occurrence of tunneling induced transparency, as shown in Fig. 3(b). As we continue to switch on the optomechanical interaction in the optomechanical cavity a_2 and keep no interaction between the NMR and qubit, the additional optomechanical coupling will cause the transition $|N_1,N_2+1,n\rangle \leftrightarrow |N_1,N_2,n+1\rangle$, which breaks down the symmetry of the tunneling induced transparency and produces a spectrally sharp absorption peak to split the single transparency window into two, i.e., the double OMIT is presented in Fig. 3(c).[45] When the strong J-C coupling interaction between NMR and qubit is added and the frequency of NMR resonates with the transition frequency between the upper and lower energy levels of qubit, the state $|N_1,N_2,n+1\rangle$ is split into both dressed states, i.e., $|N_1,N_2,n+1_+\rangle$ with the frequency ω_m+g and $|N_1,N_2,n+1_-\rangle$ with the frequency ω_m-g. $|n+1_\pm\rangle$ represent the dressed state introduced by the strong coupling between the qubit and the single-phonon state, i.e., $|N_1,N_2,n+1_\pm\rangle = (|N_1,N_2,n+1_+\rangle + |N_1,N_2,n+1_-\rangle)/\sqrt{2}$.[48] When a strong control field and a weak probe field are injected into the optomechanical cavity a_2, the beat frequency $\Delta = \omega_p - \omega_c$ resonates with the effective NMR. This will produce Stokes and anti-Stokes scattering due to the radiation pressure. The anti-Stokes fields with frequencies $\omega_{as,1} = \omega_c + (\omega_m + g)$ and $\omega_{as,2} = \omega_c + (\omega_m - g)$ are enhanced by the near-resonant cavity field, while the Stokes fields are actively suppressed because of off-resonant the cavity field.[44,49] In this case, the destructive interference between the degenerate probe field and the generated anti-Stokes fields leads to the transmission spectrum in Fig. 3(d).

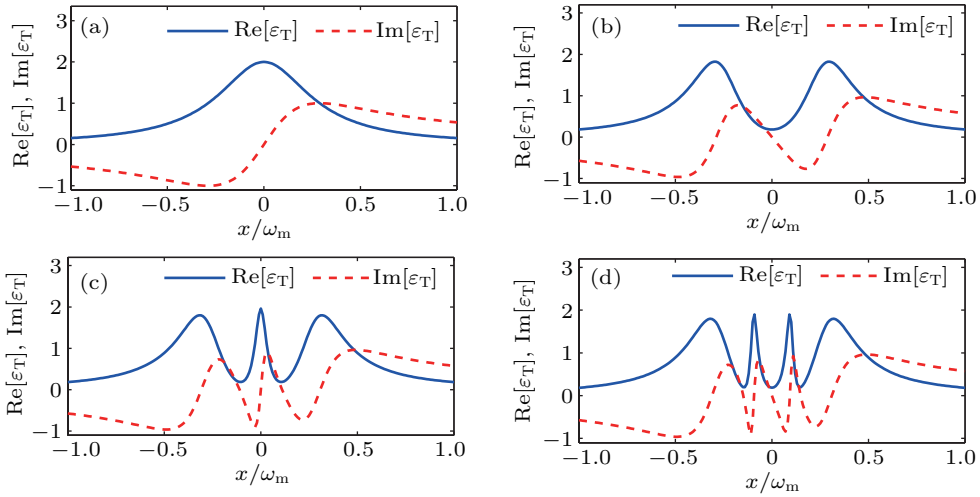


Fig. 3. The absorption $\mathrm{Re}[\varepsilon_T]$ (blue-solid line) and dispersion $\mathrm{Im}[\varepsilon_T]$ (red-dotted line) as a function of x/ω_m in the different coupling cases; i.e., (a) $g = 0$, $\chi = 0$, $J = 0$; (b) $g = 0$, $\chi = 0$, $J/2\pi = 15.0$ MHz; (c) $g = 0$, $\chi/2\pi = 2.16$ kHz, $J/2\pi = 15.0$ MHz; (d) $g/2\pi = 10.0$ MHz, $\chi/2\pi = 2.16$ kHz, $J/2\pi = 15.0$ MHz. The other parameters are given as $\kappa_1/2\pi = 15$ MHz, $\kappa_2/2\pi = 1.5$ MHz, $\gamma_q/2\pi = 0.1$ MHz, $\gamma_m/2\pi = 41.0$ kHz, and $\omega_m/2\pi = 51.8$ MHz.

4. Effect of the two-level system on the output field

The two-level system here can be considered as artificial modulation systems such as qubit, quantum dot or defect inside the NMR material. When the transition frequency of the two-level system is at near resonance with the oscillation frequency of the NMR, the effect of the two-level system on the motion of NMR cannot be neglected, especially quantum properties of NMR.[40,41] Therefore, in this section we give the discussions about the effects of the two-level system (qubit) on the output field. In Fig. 4, we show that the absorption spectra of the probe field are plotted as a function of x/ω_m for different values of the qubit–NMR detuning ($\Delta_q = \omega_q - \omega_m$) and coupling strength. In the absence of the qubit–NMR coupling (i.e., $g = 0$), a symmetrical double OMIT arising from the photon tunneling and optomechanical coupling is shown in Fig. 4(a) and corresponds to the case of Fig. 2(c).[45] However, when the qubit–NMR coupling is considered, a additional transparency window appears because the two-level system introduces extra channels with the two dressed states. In the same qubit–NMR coupling cases, Figs. 4(b)–4(d) show that the symmetry of the double transparency window is broken due to the qubit–NMR strong coupling with the different detuning. In the cases of the red-detuned ω_q (i.e., $\omega_q < \omega_m$) in Fig. 4(c) and blue-detuned ω_q (i.e., $\omega_q > \omega_m$) in Fig. 4(d), the transparency window will have the corresponding redshift and blueshift by comparing it with the case of $\omega_q = \omega_m$ in Fig. 4(b).[16] As the coupling strength g increases, the width of the central transparency window will be widened as shown in Fig. 4(e) compared with Fig. 4(b). Therefore the two-level system attached on NMR can greatly effect on the frequency width and intensity of the output field by changing the coupling strength g and detuning Δ_q.

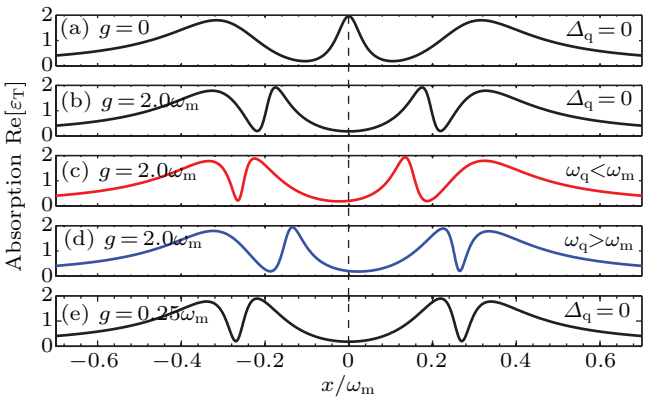


Fig. 4. The absorption $Re[\varepsilon_T]$ of the probe field as a function of x/ω_m for different values of qubit–NMR detuning and coupling strength: (a) $g = 0$, $\Delta_q = 0$; (b) $g = 0.2\omega_m$, $\Delta_q = 0$; (c) $g = 0.2\omega_m$, $\omega_q < \omega_m$; (d) $g = 0.2\omega_m$, $\omega_q > \omega_m$; (e) $g = 0.25\omega_m$, $\Delta_q = 0$. The other parameters are the same as those in Fig. 3.

Furthermore, we study the variations of the triple OMIT windows in the different cases of the laser powers of the control field and the decay rates of the two-level system. As shown in Fig. 5(a), the absorption peaks and the transparency dips on both sides move away from the center of symmetry $x/\omega_m = 0$, whereas both the center absorption peaks come closer $x/\omega_m = 0$ as the laser power value P_c increases with the fixed decay of qubit γ_q. The changes come from both the enhanced cavity fields due to the high laser power, which are different from the effects of the qubit–NMR coupling strength g in Fig. 4. The effects of the decay rate γ_q on the output field are shown when the other parameters are fixed in Fig. 5(b). We can find that the positions of absorption peaks and transparency dips remain almost unchanged in the horizontal direction, while the transparency dips get more in-depth, and the absorption peaks become higher as the decay rate γ_q decreases.

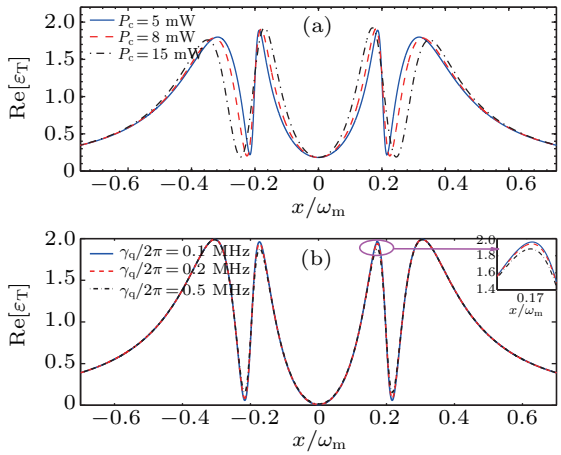


Fig. 5. The absorption $\mathrm{Re}[\varepsilon_T]$ as a function of x/ω_m in the different cases of the modulation P_c with the fixed $\gamma_q/2\pi = 0.1$ MHz in (a), the modulation γ_q with the fixed $P_c = 8$ mW. The inset in (b) is the enlarged figure around $x/\omega_m = 0.17$ MHz. The other parameters are same as those in Fig. 3.

In addition, we also study the qubit population inversion $\sigma_{z,s}$ as a function of the steady-state phonon number n. In Fig. 6, at the initial time the qubit is prepared on the ground state $|g\rangle$, the population inversion $\sigma_{z,s}$ firstly rapidly increases, then reaches a saturation value near zero when phonon number n increases. This indicates that one can modulate the population inversion $\sigma_{z,s}$ of the two-level system by the phonon number. We can find that the population inversion changes faster in the red-detuning case than the blue-detuning due to the enhanced anti-Stokes and suppressed Stokes fields.

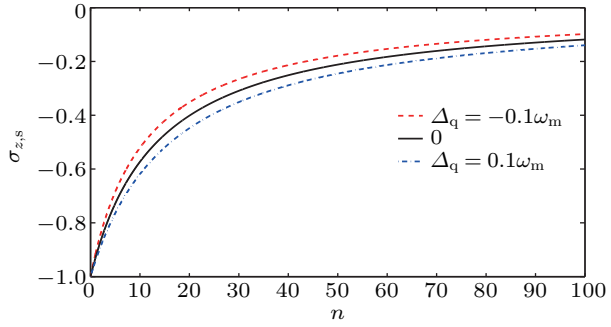


Fig. 6. The population inversion $\sigma_{z,s}$ as a function of the steady-state phonon number n. The other parameters are same as those in Fig. 3.

5. Conclusion

In summary, we have investigated the multiple-induced transparency of a hybrid optomechanical device consisting of an FP cavity tunneling coupled with an optomechanical cavity, where the end mirror of the optomechanical cavity is the NMR coupled to a two-level system. We have analyzed the physical mechanism of each transparency window by discussing the generation process of three transparency windows in detail. It is found that each of the three couplings (including photon tunneling, photomechanical and phonon–two-level system couplings) introduces a transition channel. Each of them will produce a transparent window; finally, the triple transparent windows are displayed. In addition, we focus on the effects of the two-level system on the output field and find that the qubit–NMR coupling strength can change the width of the transparency windows, and the qubit–NMR detuning can break the symmetry and change the positions of the windows. Furthermore, the effects of the laser power P_c of the control field and the decay rate γ_q of the two-level system on the transparency windows are considered. As the power P_c increases, the two transparency windows on both sides become wider, while the central transparent window becomes narrower. Although the decay rate γ_q decreases, the position of the absorption spectrum peak is slightly changed, and γ_q has only a slight effect on the width of the middle transparent window. In addition, we discuss the relations between the population inversion of the qubit and the steady-state phonon number in the different detuning Δ_q cases.

References

[1] Aspelmeyer M, Kippenberg T J and Marquardt F 2014 *Rev. Mod. Phys.* **86** 1391
[2] Kippenberg T J and Vahala K J 2008 *Science* **321** 1172
[3] Chan J, Alegre T P, Safavi-Naeini A H, Hill J T, Krause A, Gröblacher S, Aspelmeyer M and Painter O 2011 *Nature* **478** 89
[4] Bagheri M, Poot M, Fan L, Marquardt F and Tang H X 2013 *Phys. Rev. Lett.* **111** 213902
[5] Lü X Y, Wu Y, Johansson J R, Jing H, Zhang J and Nori F 2015 *Phys. Rev. Lett.* **114** 093602
[6] Schliesser A, Riviére R, Anetsberge G, Arcizet O and Kippenberg T J 2008 *Nat. Phys.* **4** 415
[7] Pagel Z, Zhong W C, Parker R H, Olund C T, Yao N Y and Müller H 2020 *Phys. Rev. A* **102** 013512
[8] Wang C, Lin Q and He B 2019 *Phys. Rev. A* **99** 023829
[9] Chen B, Jiang C and Zhu K D 2011 *Phys. Rev. A* **83** 055803
[10] Wu Z, Luo R H, Zhang J Q, Wang Y H, Yang W and Feng M 2017 *Phys. Rev. A* **96** 033832
[11] Fiore V, Yang Y, Kuzyk M C, Barbour R, Tian L and Wang H L 2011 *Phys. Rev. Lett.* **107** 133601
[12] Qin L G, Wang Z Y, Wu S C, Gong S Q, Ma H Y and Jing J 2014 *Opt. Commun.* **410** 102.
[13] Agarwal G S and Huang S M 2013 *Phys. Rev. A* **85** 021801
[14] Qin L Q, Wang Z Y, Ma H Y, Zhang C M, Ren L, Wang L L and Gong S Q 2019 *J. Opt. Soc. Am. B* **36** 1544
[15] Agarwal G S and Huang S M 2010 *Phys. Rev. A* **81** 041803
[16] Wang H, Gu X, Liu Y X, Miranowicz A and Nori F 2014 *Phys. Rev. A* **90** 023817
[17] Weis S, Rivière R, Deléglise S, Gavartin E, Arcizet O, Schliesser A and Kippenberg T J 2010 *Science* **330** 1520
[18] Xiong H, Si L G, Zheng A S, Yang X Y and Wu Y 2012 *Phys. Rev. A* **86** 013815
[19] Liu H, Qin L Q, Tian L J and Ma H Y 2019 *Chin. Phys. B* **28** 108502
[20] Lai D G, Wang X, Qin W, Hou B P, Nori F and Liao J Q 2020 *Phys. Rev. A* **102** 023707
[21] Yan X B 2020 *Phys. Rev. A* **101** 043820
[22] Safavi-Naeini A H, Alegre T P M, Chan J, Eichenfield M, Winger M, Lin Q, Hill J T, Chang D E and Painter O 2011 *Nature* **472** 69
[23] Li L, Nie W J and Chen A X 2016 *Sci. Rep.* **6** 35090
[24] Jiang C, Jiang L, Yu H L, Cui Y S, Li X W and Chen G B 2017 *Phys. Rev. A* **96** 053821
[25] Huang S M and Agarwal G S 2010 *Phys. Rev. A* **81** 033830
[26] Qin L G, Wang Z Y, Ma H Y and Gong S Q 2017 *Photon. Res.* **5** 481
[27] Liao J Q and Law C K 2011 *Phys. Rev. A* **83** 033820
[28] Zhang Z C, Wang Y P, Yu Y F and Zhang Z M 2018 *Opt. Express* **26** 11915
[29] Pirkkalainen J M, Damskägg E, Brandt M, Massel F and Sillanpää M A 2015 *Phys. Rev. Lett.* **115** 243601
[30] Yang J Y, Wang D Y, Bai C H, Guan S Y, Gao X Y, Zhu A D and Wang H F 2019 *Opt. Express* **27** 22855
[31] Qin L Q, Wang Z Y, Lin G W, Zhao J Y and Gong S Q 2016 *IEEE J. Quantum. Electron.* **53** 9300106
[32] Gu W J, Yi Z, Sun L H and Yan Y 2018 *Opt. Express* **26** 30773.
[33] Bøkje K 2019 *Phys. Rev. A* **99** 023858
[34] Li G L and Wang X G 2018 *Phys. Rev. A* **98** 013803
[35] Zhang F Y, Yan W B and Yang C P 2018 *Phys. Rev. A* **98** 042331
[36] Xiong W, Jin D Y, Jing J, Lam C H and You J Q 2015 *Phys. Rev. A* **92** 032318
[37] Tian L 2005 *Phys. Rev. B* **72** 195411
[38] Wang X, Miranowicz A, Li H R and Nori F 2016 *Phys. Rev. A* **93** 063861
[39] Tian L 2011 *Phys. Rev. B* **84** 035417
[40] Ramos T, Sudhir V, Stannigel K, Zoller P and Kippenberg T 2013 *Phys. Rev. Lett.* **110** 193602
[41] He Q, Badshah F, Zhang H Y, Ali H, Basit A, Hu Y and Ge G Q 2019 *Laser Phys. Lett.* **16** 035202
[42] Cotrufo M, Fiore A and Verhagen E 2017 *Phys. Rev. Lett.* **118** 133603
[43] Wang H, Gu X, Liu Y X, Miranowicz A and Nori F 2015 *Phys. Rev. A* **92** 033806
[44] Jiang L, Yuan X R, Cui Y S, Chen G B, Zuo F and Jiang C 2017 *Phys. Lett. A* **381** 3289
[45] Gu W J and Yi Z 2014 *Opt. Commun.* **333** 261
[46] Xiong W, Jin D Y, Qiu Y, Lam C H and You J Q 2016 *Phys. Rev. A* **93** 023844
[47] Ullah Q, Jing H and Saif F 2018 *Phys. Rev. A* **97** 033812
[48] Liu Y L, Wu R, Zhang J, Özdemir K, Yang L, Nori F and Liu Y X 2017 *Phys. Lett. A* **95** 013843
[49] Xiong H and Wu Y 2008 *Appl. Phys. Rev.* **5** 0301305